



REACTION PATHS AND ELEMENTARY BIFURCATIONS TRACKS: THE DIABATIC 1B_2 -STATE OF OZONE

S. C. FARANTOS

*Institute of Electronic Structure and Laser,
Foundation for Research and Technology-Hellas, and
Department of Chemistry, University of Crete,
Iraklion 711 10, Crete, Greece*

ZHENG-WANG QU, H. ZHU and R. SCHINKE
*Max-Planck-Institut, Dynamik und Selbstorganisation,
D-37073 Göttingen, Germany*

Received November 5, 2004; Revised March 15, 2005

Bifurcations of equilibrium points and periodic orbits are common in nonlinear dynamical systems when some parameters change. The vibrational motions of a molecule are nonlinear, and the bifurcation phenomena are seen in spectroscopy and chemical reactions. Bifurcations may lead to energy localization in specific bonds, and thus, they have important consequences for elementary chemical reactions, such as isomerization and dissociation/association. In this article we investigate how elementary bifurcations, such as saddle-node and pitchfork bifurcations, appear in small molecules and show their manifestations in the quantum mechanical frequencies and in the topology of wave functions. We present the results of classical and quantum mechanical calculations on a new (diabatic) potential energy surface of ozone for the 1B_2 state. This excited electronic state of ozone is pertinent for the absorption of the harmful UV radiation from the sun. We demonstrate that regular localized overtone states, which extend from the bottom of the well up to the dissociation or isomerization barrier, are associated with families of periodic orbits emanated from elementary bifurcations.

Keywords: Bifurcation theory; periodic orbits; classical and quantum molecular dynamics.

1. Introduction

Understanding the dynamics of molecules at energies where chemical bonds break or are formed is not only of academic importance but basically it is the foundation of chemistry. In the Born–Oppenheimer approximation for the separation of the electronic and nuclear motions in a molecule, Quantum Chemistry answers in part this problem by solving the electronic Schrödinger equation to produce molecular potential energy surfaces (PES). The solution of the nuclear equations of motion is required to understand the elementary

chemical processes, such as isomerization and dissociation/ association. Since elementary chemical reactions require the excitation of the molecule to high energy vibrational-rotational states, spectroscopic methods which capture the molecule at these extreme motions are applied, together with theoretical methods to assign the spectral lines and to extract the dynamics.

In the second half of the twentieth century several vibration-rotation molecular spectroscopic methods were developed which allowed one to record high resolution spectra of highly excited

states. Among them the Stimulated Emission Pumping (SEP) and the Dispersed Fluorescence (DF) spectroscopy [Dai & Field, 1995] gave an impetus to the field of vibrationally excited molecules in the ground electronic state. SEP is a double-resonance technique. A first laser promotes the molecule to a single rovibrational level of an electronically excited state, while a second laser stimulates the emission down to a highly excited vibrational state of the ground electronic state. Due to the improved Franck–Condon access for transitions corresponding to a significant change of molecular geometry, SEP gives access to a class of vibrational states which are not accessible by direct overtone spectroscopy. Molecules studied by SEP and DF spectroscopy are C₂H₂ [Jacobson *et al.*, 1998a, 1998b, 1999], HCP [Ishikawa *et al.*, 1998], SO₂ [Yamanouchi *et al.*, 1990, 1988; Sako & Yamanouchi, 1996], HFCO [Yamamoto & Kato, 1998], HCO [Keller *et al.*, 1996], DCO [Keller *et al.*, 1997], HCN [Northrup *et al.*, 1997] and NO₂ [Delon *et al.*, 2000]. Since the SEP and DF methods excite the molecule at very high vibrational states, they are ideal spectroscopic techniques to deduce the dynamics close to the isomerization or dissociation threshold. As a matter of fact, the SEP spectra of acetylene were the first which revealed vibrational (quantum) chaos at energies above the isomerization threshold of acetylene to vinylidene [Jonas *et al.*, 1993].

Other high resolution spectroscopic methods which have contributed to the detailed study of small polyatomic molecules are the High Resolution Fourier Transform and Laser Spectroscopy in several diversities: Frequency Modulation with Diode Lasers (FMDL), Cavity Ringdown Spectroscopy (CRDS), Intracavity Laser Absorption Spectroscopy (ICLAS), Optoacoustic (OA) and Optothermal Spectroscopy, and Photofragment Spectroscopy. Several molecules have been studied, such as H₂O, HO₂, CO₂, HCN, HNO, N₂O, OCS, HOCl, HCO, CH₄, C₆H₆, NH₃, HOOH, s-tetrazine, dimethyl-s-tetrazine pyridine, propyne to mention a few. A short description of these methods are presented in [Herman *et al.*, 1999]. Crim and coworkers [1999] have combined the photoacoustic spectroscopy with a time of flight apparatus to control the products in unimolecular and bimolecular reactions by vibrationally exciting specific chemical bonds of reactant molecules. This bond selective chemistry reveals energy localization in specific bonds.

Laser femtosecond spectroscopy and molecular beams have allowed to study isolated molecules and follow a chemical reaction in real time. This requires the simultaneous development of theoretical models to interpret the experimental results. The established theoretical methods based on a normal mode description of the molecular vibrations, applied at energies close to the equilibrium point, are not valid for highly vibrationally excited molecules. The deviation from the harmonic approximation of the potential energy surface imposes the need for the construction of accurate potential functions that describe several and energetically accessible reaction channels. These are nonlinear functions and the application of nonlinear mechanics to investigate the dynamics of the molecule is necessary. Polyatomic molecules stimulate new computational challenges in solving accurately the Schrödinger equation and obtaining hundreds of vibrational states. Nowadays, triatomic molecules can be treated with fully *ab initio* methods, both in their electronic and nuclear parts. Tetratomic molecules are more difficult to deal with, in spite of the progress which has recently been achieved. For example, six-dimensional calculations up to energies of the isomerization of acetylene to vinylidene have been published [Zou & Bowman, 2002].

Apart from the computational challenges small polyatomic molecules unravel conceptual and physical interpretation problems. A result of the nonlinear mechanical behavior of a dynamical system at high energies is the simultaneous appearance of ordered motions and chaos, as well as the genesis of new types of motions via bifurcation phenomena. *What are the quantum mechanical counterparts of these classical behaviors? What are the spectroscopic fingerprints of the nonlinear dynamics in the molecules? In cases where the vibrational spectra depict isomerization and dissociation processes how can we identify them in the spectra?* As a matter of fact, the progress of nonlinear mechanics forces us to re-examine the mechanisms of the breaking and/or forming of a single chemical bond as it occurs in elementary chemical reactions. To answer the above questions new assignment schemes which allow the classification of quantum states in a meaningful and useful way are required and such novel methods have been developed thanks to the theory of periodic orbits (PO), their bifurcations [Wiggins, 2003] and semiclassical theory [Gutzwiller, 1990].

The theory of periodic orbits plays a dominant role in the formulation of classical mechanics. However, what makes periodic orbits important for molecules are the advances obtained in semiclassical theory in the past years. Gutzwiller [1990] using Feynman's path integral formulation has derived a semiclassical expression for the trace of the resolvent (Green operator) of the quantum Hamiltonian operator as a sum over all isolated periodic orbits, taking into account their linear stability indices. This formula provides approximate values for the quantum eigenenergies of classically chaotic systems. Berry and Tabor [1977] derived in a different way the trace formula based on the Einstein–Brillouin–Keller quantization rule. Their formula gives the quantum density of states as a coherent summation over resonant tori, and therefore it is applicable to integrable systems. Finally, a uniform result bridging the Berry–Tabor and Gutzwiller trace formulas for the case of a resonant island chain was derived by Ozorio de Almeida [1990]. Last but not least, the importance of periodic orbits for a qualitative understanding of the localization of quantum mechanical eigenfunctions in configuration space came from the scarring theory of Heller [1984]. It turns out, that for small polyatomic molecules the probability density of eigenfunctions is accumulated along short-period stable or the least unstable periodic orbits. In some cases, such as overtone states, we can associate isolated PO with specific eigenfunctions.

Periodic orbits evolve with the energy of the system or any other parameter in the Hamiltonian, bifurcate and produce new periodic orbits which portrait the resonances among the vibrational degrees of freedom. Generally, PO reveal the structure of phase space at different energies, i.e. the different types of motions. We can apply these methods with two different strategies. In the first one we follow the *Global-approach*, that is we employ global potential energy surfaces valid over the complete nuclear configuration space from the minima to the dissociation/isomerization channels and compute families of periodic orbits from the minima of the potential up to and above the dissociation threshold or up to the energy where they are annihilated.

The second strategy, named the *patch-approach*, is usually applied by spectroscopists. An effective Hamiltonian is fitted to spectroscopic results reproducing part of the vibrational energy spectrum, and thus a patch of the global

Hamiltonian. The spectroscopic Hamiltonians, which are mainly of reduced type (less degrees of freedom) incorporate the resonance(s) among the frequencies of two different degrees of freedom observed in experimental spectra. These Hamiltonians can be extended to fit calculated spectra and then a PO analysis is carried out in a similar fashion as in the *Global-approach*.

We have systematically studied the PO continuation/bifurcation (C/B) diagrams for several types of molecules; triatomic [Farantos, 1996] and tetratomic [Prosmiiti & Farantos, 1995, 2003] molecules, van der Waals molecules [Guantes *et al.*, 1999] and at energies below and above dissociation threshold [Founargiotakis *et al.*, 1997]. Similarly to the landscape of the PES which reveals the relative stability/instability and reactivity of the molecular isomers, the families of periodic orbits portray the structure of phase space at specific energies, and they thus reveal the dynamics of the molecule at least around the periodic orbits. It is now accepted that the regular motions and the chaotic motions in phase space consist of highly complicated entangled networks. Periodic orbits depicted by a C/B diagram may be considered as providing a higher order of approximation to the dynamics of the molecule, after obtaining the zero order approximation with the potential function.

The landscape of the PES may drastically change as energy increases in the molecule. Barriers and minima may disappear/appear. Similarly, the phase space changes with the total energy. Stable, quasiperiodic motions may turn to unstable chaotic ones and vice versa. But most importantly, via the bifurcations of periodic orbits new types of motion may emanate. The bifurcation theory of Hamiltonian dynamical systems has mainly been developed in the last half of twentieth century. One important outcome of the theory is the identification of the elementary bifurcations which are described by very simple Hamiltonians. In spite of their simplicity they can also describe a complex dynamical system close to particular critical energies. This makes elementary bifurcations generic. For molecular Hamiltonian systems we have identified the saddle-node, pitchfork and Hopf-like elementary bifurcations.

Bifurcation phenomena, i.e. the change of the structure of the orbits by varying one or more parameters, are well known in vibrational spectroscopy. For example, the transition from normal to local mode oscillations, first discovered

in symmetric ABA molecules, is related to the elementary *pitchfork* bifurcation [Halonen, 1998; Lawton & Child, 1981; Prosmiiti *et al.*, 1999]. In what follows we show that localization of energy is also obtained via another generic bifurcation of periodic orbits, the saddle-node (SN). Periodic orbits which emerge from SN bifurcations appear abruptly at some critical value of the energy, usually in pairs, and change drastically the phase space around them. They penetrate in regions of nuclear phase space which the normal mode motions cannot penetrate. Saddle-node bifurcations are of generic type, i.e. they are robust and remain for small (perturbative) changes of the potential function [Prosmiiti & Farantos, 1995, 2003].

We initially determined the importance of SN bifurcations of periodic orbits in studies of the isomerization dynamics in double well potential functions [Farantos, 1993]. These PO connect the two minima and scar the isomerizing wave functions, i.e. eigenfunctions with significant probability density in both wells. Their birth is due to the unstable periodic orbit which emanates from the saddle point of the potential energy surface. However, even below the potential barrier a series of SN bifurcations of periodic orbits pave the way to the isomerization process. The spectroscopic signature of such SN bifurcations has been found in a number of triatomic molecules [Ishikawa *et al.*, 1999; Joyeux *et al.*, 2002]. HCP was the first molecule where experimental evidence for SN bifurcations was given. In the other extreme, infinite dimensional systems, such as periodic or random lattices, show spatially localized and periodic in time motions, called *discrete breathers (DB)*, and it has been shown that they can also be associated with saddle-node bifurcations [Flach & Willis, 1998; Kopidakis & Aubry, 1999]. Spectroscopic evidence for the existence of discrete breathers can be found among biomolecules [Xie *et al.*, 2000].

In the present article we apply PO analysis to an electronically excited state of ozone. In Sec. 2 we introduce the concepts of elementary bifurcations and show how saddle-node bifurcations emerge via simple one-dimensional Hamiltonians, which however, depict the dynamics on the complicated molecular potential energy surfaces. In Sec. 3 we present our strategy to locate periodic orbits in multidimensional Hamiltonians and for general coordinate systems. Section 4 describes the results on the excited ${}^1\text{B}_2$ electronic state of ozone. We conclude with Sec. 5.

2. Elementary Bifurcations

We call elementary those bifurcations which can appear in the simplest one- or two-dimensional nonlinear systems by varying one or two parameters. Comparing these systems with the complicated multidimensional molecular Hamiltonians, we may think that a simple one-dimensional Hamiltonian is only of pedagogical use. This is not true, since we can show that at the critical value of the parameter at which the bifurcation occurs, the system can be reduced to one of lower dimension by using the central manifold theorem [Wiggins, 2003], and then we can describe it with a simple Hamiltonian by transforming to normal forms. The mathematical theory of bifurcations in dynamical systems is well developed and there are excellent books [Guckenheimer & Holmes, 1983; Wiggins, 2003] and review articles [Crawford, 1991] to introduce the subject. In this section we discuss how a saddle-node bifurcation appears in the simplest nonlinear Hamiltonians, that with a cubic and quartic potential.

2.1. Cubic potentials

For a system of one degree of freedom with a Hamiltonian

$$H(q, p) = \frac{1}{2}p^2 + V(q) \quad (1)$$

the Hamilton's equations of motion for a conservative vector field are

$$\dot{q} = \frac{\partial H}{\partial p} \quad (2)$$

$$\dot{p} = -\frac{\partial H}{\partial q}. \quad (3)$$

q is the generalized coordinate, p its conjugate momentum and $V(q)$ the potential function. The stationary points of the potential, i.e. $dV(q)/dq = 0$, are the equilibrium (or fixed) points of the vector field; $\dot{q} = \dot{p} = 0$. The above mentioned books [Guckenheimer & Holmes, 1983] describe the elementary bifurcations of fixed points of vector fields. Here, we do not attempt a complete cover of this subject but we discuss mainly those cases which are related to the saddle-node bifurcations.

We assume a general cubic potential

$$V(q) = \frac{1}{3}q^3 - \frac{1}{2}\alpha q^2 - \beta q - \gamma \quad (4)$$

The equilibrium points of Hamilton equations are then the roots of the second order polynomial

$$\frac{dV(q)}{dq} = q^2 - \alpha q - \beta = 0. \quad (5)$$

The discriminant of the above equation is defined as

$$D = \alpha^2 + 4\beta. \quad (6)$$

In order that Eq. (5) has two real roots (equilibrium points) $D \geq 0$ is required. Thus, the parabola $D = 0$ defines the region in the two-parameter space, (β, α) , where these two roots exist. Figure 1 exhibits this region and Fig. 2 shows the evolution

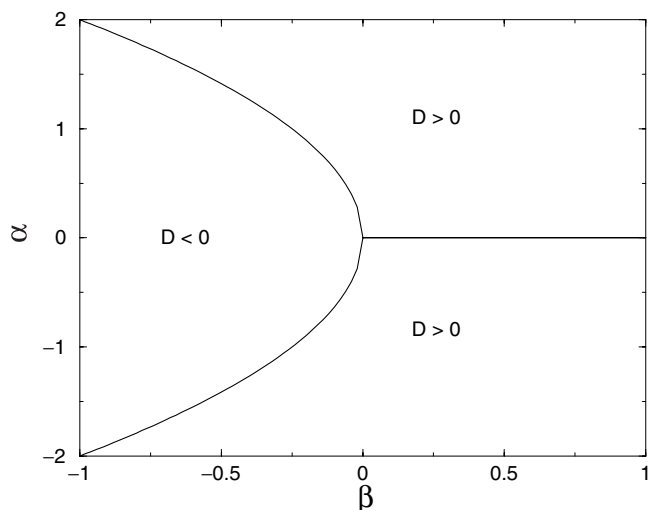


Fig. 1. The sign of the discriminant D [Eq. (6)] in the parameter space (β, α) of a cubic potential.

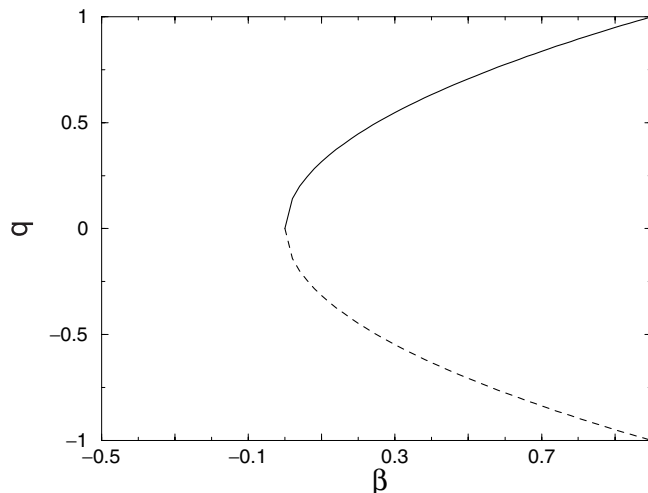


Fig. 2. C/B diagram of a cubic potential. The coordinates q of the two equilibria are shown as function of the parameter β and $\alpha = 0$. Continuous line denotes the stable equilibrium point (minimum) and the dashed line the unstable equilibrium point (maximum).

of the two equilibria of the potential by varying the parameter β assuming $\alpha = 0$. This graph is a typical saddle-node continuation/bifurcation diagram. We notice, that there are no equilibrium points for negative values of β and at $\beta = 0$ the double root signals the genesis of the saddle-node bifurcation. The two branches correspond to stable (solid line) and to unstable (dashed line) equilibrium points. Stable means that trajectories close to this point will remain in the nearby region, whereas unstable points mean that nearby trajectories will deviate from it. Visualization of the equilibrium points of the corresponding potential function explains better the stable and unstable terms. Such a plot is shown in Fig. 3 for several values of β .

In this figure we can distinguish three different regimes. For $\beta < 0$ there are no equilibrium points, for $\beta > 0$ there are two equilibrium points, one minimum and one maximum, and for $\beta = 0$ (dashed line) there is one saddle point at $q = 0$. In Fig. 4 several trajectories are plotted in the phase plane, (q, p) , and for $\beta = 1$. The dashed line denotes the separatrix of the two types of motions allowed for this dynamical system; closed stable orbits and unbound orbits. This phase space graph is typical of a saddle-node bifurcation. It is important to emphasize that the structure of phase space does not change qualitatively by introducing a second

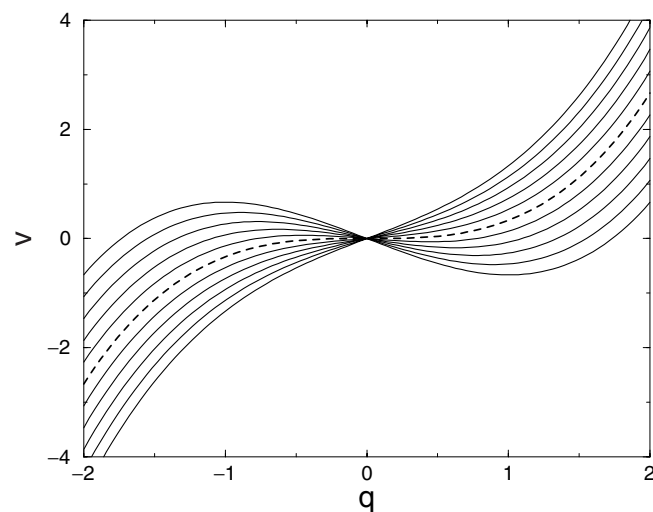


Fig. 3. Plots of a cubic potential for several values of β . For $\beta < 0$ there are no equilibrium points, for $\beta > 0$ there are two equilibrium points, one minimum and one maximum, and for $\beta = 0$ (dashed line) there is one saddle point at $q = 0$.

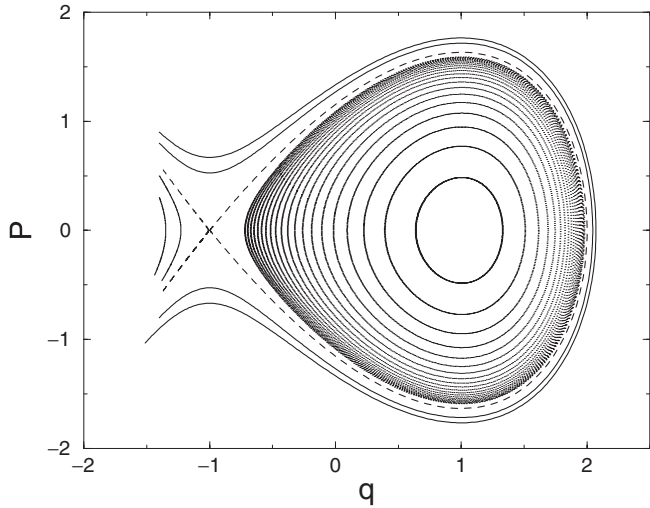


Fig. 4. Trajectories which portray the phase space structure in the region of a saddle-node bifurcation ($\beta = 1$).

parameter. The C/B diagram remains the same with two branches for values of $\alpha \neq 0$.

2.2. Quartic potentials

A general quartic potential is

$$V(q) = \frac{1}{4}q^4 - \frac{1}{3}\alpha q^3 - \frac{1}{2}\beta q^2 - \gamma q - \delta \quad (7)$$

The equilibrium points are:

$$\frac{dV(q)}{dq} = q^3 - \alpha q^2 - \beta q - \gamma = 0. \quad (8)$$

This cubic equation can be reduced to a two parameter equation with the transformations

$$x = q - \frac{\alpha}{3} \quad (9)$$

$$\mu = \frac{\alpha^3}{3} + \beta \quad (10)$$

$$\lambda = \frac{2\alpha^3}{27} + \frac{\alpha\beta}{3} + \gamma. \quad (11)$$

The reduced cubic polynomial is

$$x^3 - \mu x - \lambda = 0. \quad (12)$$

The discriminant is defined by

$$D = -\frac{\mu^3}{27} + \frac{\lambda}{4}. \quad (13)$$

The roots of Eq. (12) are:

- (i) For $D > 0$, one real root and two imaginary.
- (ii) For $D < 0$, three different real roots.

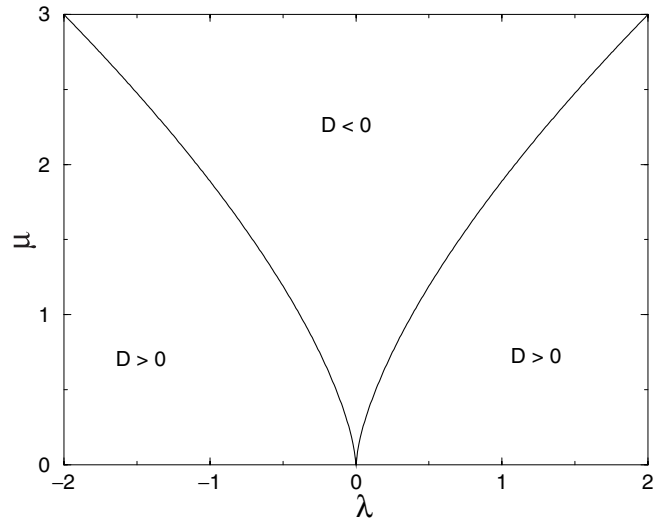


Fig. 5. The sign of the discriminant D [Eq. (13)] in the parameter space (λ, μ) of a quartic potential.

- (iii) For $D = 0$, three real roots two of them being equal. Figure 5 presents the sign of the discriminant in the parameter space (λ, μ) . The cusp curve defines the values of (λ, μ) where the discriminant is zero. Thus, crossing this curve from positive to negative values of D we pass from one to three equilibrium points. A double degeneracy of equilibrium points is encountered at the cusp curve.

The C/B diagram for $\lambda = 0$ and varying the parameter μ is shown in Fig. 6. This is a typical pitchfork bifurcation. The introduction of a second parameter ($\lambda \neq 0$) results in the C/B

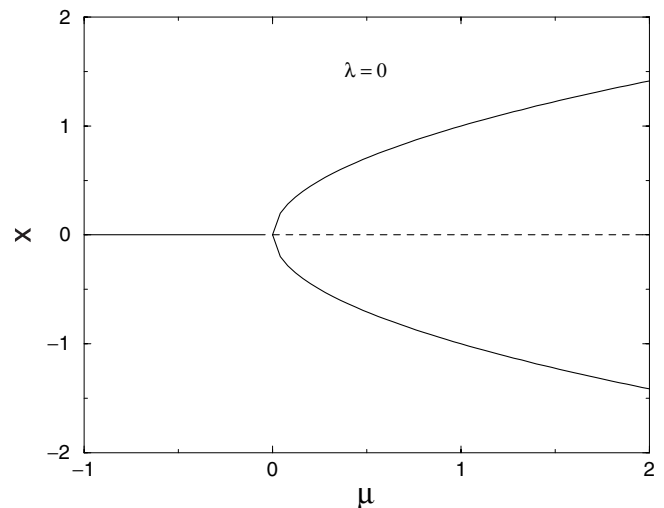


Fig. 6. C/B diagram of a quartic potential and for $\lambda = 0$ (pitchfork bifurcation). Continuous lines denote stable equilibria and dashed line the unstable equilibrium point.

diagram shown in Fig. 7. Comparing the two continuation/bifurcation diagrams for $\lambda = 0$ and $\lambda \neq 0$ (Figs. 6 and 7), we can see that the unstable branch in the pitchfork bifurcation (dashed line) becomes the unstable branch of a saddle-node bifurcation, whereas one stable branch in the pitchfork bifurcation is the stable branch of the SN bifurcation. We can also see that the parent family in the pitchfork bifurcation turns to a *hysteresis*. We can think of this continuation/bifurcation diagram as a folded surface in the (λ, μ, x) space. The size of the gap in the C/B curves with the parameter μ depends on the value of the parameter λ . Increase of λ results in an increase of the gap (see Fig. 8).

The three equilibria in the quartic potential are two minima and one maximum. In Fig. 9 we

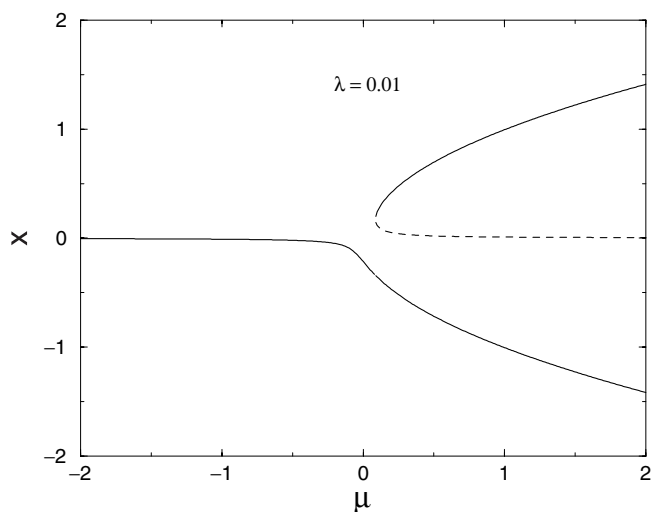


Fig. 7. As in Fig. 6 but for $\lambda = 0.01$. A saddle-node and a hysteresis bifurcation appear.

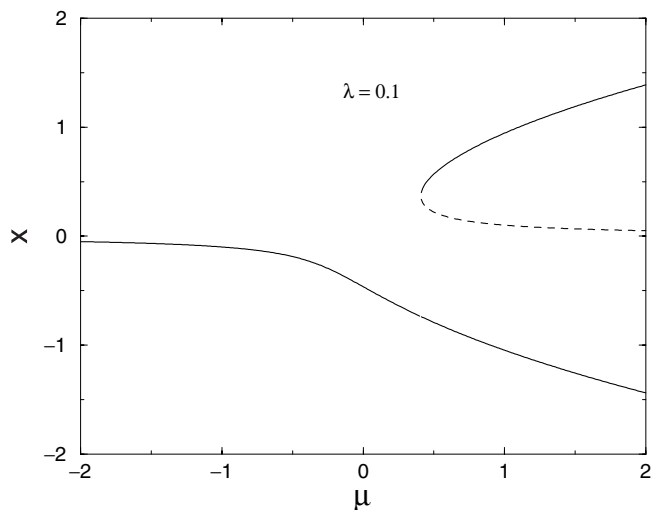


Fig. 8. As in Fig. 6 but for $\lambda = 0.1$.

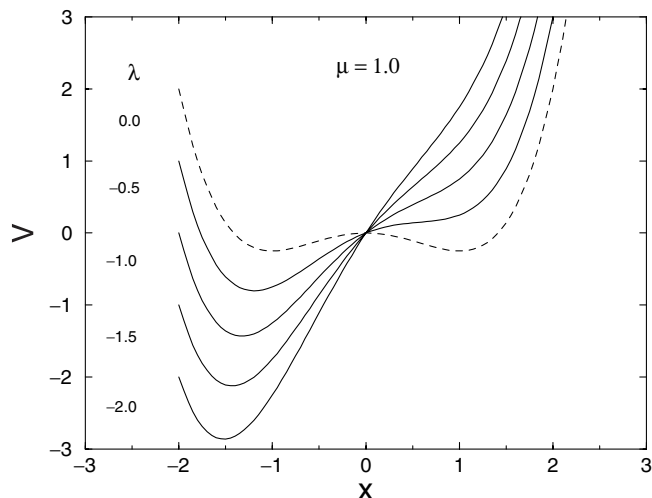


Fig. 9. Potential curves of a quartic potential and for several values of λ . The dashed line is the symmetric double well potential ($\lambda = 0$).

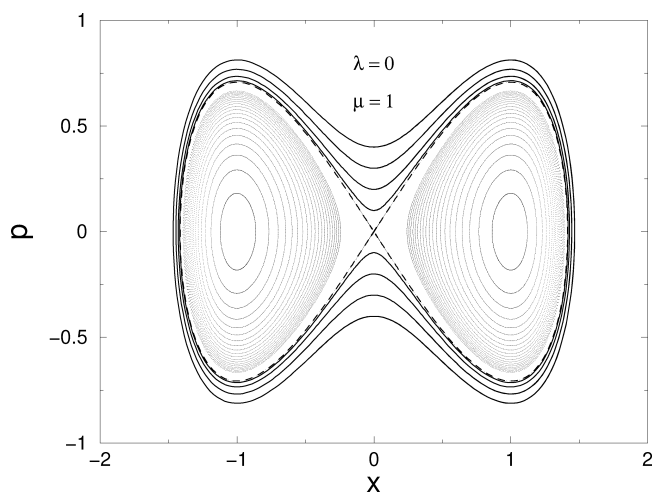


Fig. 10. Phase space structure of a symmetric double well quartic potential.

plot potential curves for several values of λ and for $\mu = 1$. As λ approaches zero the kink in the potential is transformed to a double well.

Trajectories plotted in the phase plane (x, p) are shown in Fig. 10 for the symmetric double well potential ($\lambda = 0$ and $\mu = 1$). The separatrix (dashed line) emanates from the maximum of the potential, and it separates the two types of motions encountered in this system.

3. Bifurcations of Periodic Orbits

The phase space structure of a dynamical system is determined by locating stationary objects, such as

(i) equilibrium points, (ii) periodic orbits, (iii) tori, (iv) reduced dimension tori, and (v) stable and unstable manifolds [Guckenheimer & Holmes, 1983; Wiggins, 2003].

Equilibrium points and periodic orbits located for a range of energies or any other parameter, are a good starting point to portrait the structure of phase space of small molecules. This has been demonstrated by studying together the classical and quantum mechanics for several triatomic molecules [Farantos, 1996; Ishikawa *et al.*, 1999; Joyeux *et al.*, 2002; Joyeux *et al.*, 2005]. If a global PES is available in a curvilinear coordinate system for the molecule, we need general and robust algorithms to locate periodic solutions of the equations of motion. This problem is formulated as follows.

If $H(\mathbf{q}, \mathbf{p})$ is the Hamiltonian of a system with N degrees of freedom, the equations of motion are written in Hamilton's form as,

$$\begin{aligned} \frac{dq_i}{dt} &= \dot{q}_i(t) = \frac{\partial H}{\partial p_i} \\ \frac{dp_i}{dt} &= \dot{p}_i(t) = -\frac{\partial H}{\partial q_i}, \quad i = 1, \dots, N. \end{aligned} \quad (14)$$

q_i , $i = 1, \dots, N$, are the generalized coordinates and p_i , $i = 1, \dots, N$, their conjugate momenta. The symplectic properties [Arnold, 1980] of these equations are better shown by considering coordinates and momenta as the components of the generalized coordinate vector \mathbf{x} ,

$$\mathbf{x} = (q_1, \dots, q_N, p_1, \dots, p_N)^+, \quad (15)$$

where $+$ denotes the transpose of the $2N$ -D column vector. The equations of motion are then written,

$$\dot{\mathbf{x}}(t) = J \frac{\partial H(\mathbf{x})}{\partial \mathbf{x}} \equiv J \partial H(\mathbf{x}) \equiv J \nabla H(\mathbf{x}), \quad (16)$$

where J is the symplectic matrix,

$$J = \begin{pmatrix} 0_N & I_N \\ -I_N & 0_N \end{pmatrix}. \quad (17)$$

0_N and I_N are the zero and unit $N \times N$ matrices, respectively. $J \nabla H(\mathbf{x})$ is a vector field, and J satisfies the relations,

$$J^{-1} = -J \quad \text{and} \quad J^2 = -I_{2N}. \quad (18)$$

To locate in general stationary objects we solve a two-point boundary value problem, i.e. we want to find those specific trajectories which satisfy at

two different times $t = 0$ and $t = T$ a relation

$$B[\mathbf{x}(0), \mathbf{x}(T)] = 0. \quad (19)$$

For example, to find periodic orbits we impose the following two-point boundary conditions

$$\mathbf{x}(T) - \mathbf{x}(0) = 0, \quad (20)$$

where T is the period of time after which the trajectory by integrating the equations of motion returns to its initial point in phase space, $\mathbf{x}_0 = \mathbf{x}(0)$.

The equilibrium points are defined by requiring $\dot{\mathbf{x}} = 0$, or

$$\nabla H(\mathbf{x}) = 0. \quad (21)$$

Since $\dot{\mathbf{x}}(T) = \dot{\mathbf{x}}(0)$, we can see that the equilibrium points are also solutions of Eq. (20).

To locate PO for a specific period T we study the linearized system based on the Hartman–Grobman theorem [Guckenheimer & Holmes, 1983] which states that there is a continuous change of coordinates that relates the linearization to the vector field ($J \nabla H(\mathbf{x})$). Thus, important conclusions obtained from the linearized system apply to the nonlinear one as well.

If $\mathbf{x}(t)$ is a solution of Eq. (16) we want to know the behavior of a nearby trajectory

$$\mathbf{x}'(t) = \mathbf{x}(t) + \zeta(t). \quad (22)$$

From Eq. (16) we have,

$$\dot{\mathbf{x}}'(t) - \dot{\mathbf{x}}(t) = J \nabla H(\mathbf{x}') - J \nabla H(\mathbf{x}). \quad (23)$$

A Taylor expansion of the rhs of Eq. (23) up to the first order gives,

$$\dot{\zeta}(t) = J \partial^2 H(\mathbf{x}(t)) \zeta(t). \quad (24)$$

$\partial^2 H(\mathbf{x}(t))$ denotes the matrix of second derivatives of the Hamiltonian evaluated at the original trajectory $\mathbf{x}(t)$ for time t .

If,

$$A(t) = J \partial^2 H(\mathbf{x}(t)),$$

then Eq. (24) is written as,

$$\dot{\zeta}(t) = A(t) \zeta(t). \quad (25)$$

These are $2N$ linear differential equations with time dependent coefficients, and they are called *variational equations*.

The general solution of Eq. (25) can be expressed by evaluating the fundamental matrix at time t , $Z(t)$ [Yakubovich & Starzhinskii, 1975]. This is the matrix with columns vectors

$(1, 0, \dots, 0), (0, 1, 0, \dots, 0), \dots, (0, 0, \dots, 1)$ at $t = 0$, i.e.

$$Z(0) = I_{2N}. \quad (26)$$

The general solution of Eq. (24) is then given by,

$$\zeta(t) = Z(t)\zeta(0), \quad (27)$$

where $\zeta(0)$ describes the initial displacement from the trajectory \mathbf{x}_0 . The fundamental matrix satisfies the variational equations as can be easily proved;

$$\dot{Z}(t) = A(t)Z(t). \quad (28)$$

Thus, by solving Eqs. (16) and (28) we obtain the trajectory with the chosen initial conditions and the behavior of the nearby trajectories at the linear approximation.

For periodic orbits the fundamental matrix at $t = T$,

$$M = Z(T) = \frac{\partial \mathbf{x}(T)}{\partial \mathbf{x}_0}, \quad (29)$$

is called monodromy matrix, the eigenvalues of which determine the stability of periodic orbit [Wiggins, 2003]. Because of the symplectic property of Hamiltonian systems if λ_i is an eigenvalue of the monodromy matrix, then its complex conjugate λ_i^* , as well as the λ_i^{-1} and $(\lambda_i^{-1})^*$ are also eigenvalues. The properties of the monodromy matrix and the different cases of stability have been described before [Farantos, 1992]. For a system of three degrees of freedom the eigenvalues and thus the kinds of stability are represented in Fig. 11. As energy varies, the eigenvalues of stable periodic orbits move on the unit complex circle. When the eigenvalues are out of the unit circle but on the real axis the periodic orbit is single or double unstable, and finally four complex eigenvalues out of the unit circle characterize a complex unstable PO.

Stationary points and periodic orbits are located numerically with a new version of POMULT program written in Fortran95 [Farantos, 1998]. We apply multiple shooting methods which convert the two-point boundary value problem to m -initial value problems, i.e. we search for the appropriate initial values of coordinates and momenta which satisfy the boundary conditions and the continuity equations [Farantos, 1998] which guarantee a smooth orbit. Analytic first and second derivatives of the potential function required for the solution of the equations of motion and the variational equations are computed by the AUTO-DERIV, a Fortran

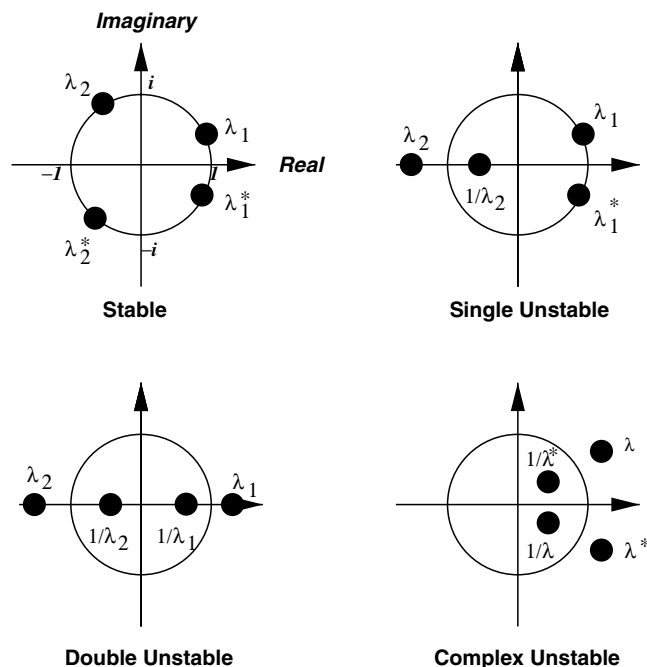


Fig. 11. Eigenvalues of the monodromy matrix for a molecule with three degrees of freedom. There are three pairs of complex conjugate eigenvalues one of which is always equal to one (not shown). The other two pairs move in the complex plane as energy varies. The positions of these eigenvalues with respect to the complex unit circle determine the stability of the PO.

code for automatic differentiation of an analytic function of many variables written in Fortran [Stamatiadis *et al.*, 2000].

4. Application to the 1^1B_2 -State of Ozone

Ozone is an important molecule for atmospheric chemistry because of its role in shielding earth from the harmful UV light. There have been numerous studies of its spectroscopy and photodissociation [Houston, 2003]. The absorption of the UV radiation excites electronically the molecule to the (2^1A_1) and the (1^1B_2) states. Recently, we have carried out theoretical *ab initio* calculations and we have shown that the two notorious absorption bands observed, Huggins and Hartley, are due to the excitation of the molecule from the ground electronic state to the (1^1B_2) state [Qu *et al.*, 2004a, 2004b]. The mechanism of the photodissociation of ozone is complicated because of the involvement of several excited states. Nevertheless, the construction of an analytical function for the diabatic (1^1B_2)

state of ozone, as well as the calculation of high quality quantum mechanical vibrational eigenfunctions up to the dissociation threshold, as a result of the previous studies, lead us to investigate further the dynamics of the molecule in this excited state. Here, we apply our periodic orbit techniques to explore the structure of phase space, and thus, to trace reaction paths on this surface.

The potential energy for the diabatic 1B_2 -state of ozone has been described in detail before [Qu *et al.*, 2004a, 2004b]. The equilibrium geometry of ozone in this excited state has a C_s symmetry, with one *long-bond* and one *short-bond*, in contrast to the ground electronic state where the minimum is of C_{2v} symmetry with two equal bonds. Because of the permutational symmetry of the molecule there are three equivalent minima and several saddle points among them. In Table 1 we tabulate the geometries and the energies of one minimum and related saddle points. The nuclear configurations are described in Jacobi coordinates, which are the distance R , of the *long-bond* oxygen atom from the center of mass of the *short-bond* end atoms whose bond length is r , and the angle γ between the vectors \mathbf{R} and \mathbf{r} (see Fig. 12). This Jacobi coordinate system is appropriate to describe the dissociation of a triatomic molecule.

All quantum mechanical calculations are for zero total angular momentum. The discrete variable representation [Light & Carrington, 2000] (DVR) is used to represent the Hamiltonian matrix. The calculations are done in symmetric-Jacobi coordinates: R' is now the distance from the central oxygen atom to the center of mass of the two end atoms, r' the distance between the two end atoms, and γ' denotes the angle between the vectors \mathbf{R}' and \mathbf{r}' . The choice of this coordinate system simplifies the quantum mechanical calculations, since the Hamiltonian is symmetric with respect to the exchange of the two end atoms, i.e. it is symmetric with respect to $\gamma' = 90^\circ$. Thus, the eigenstates are

Table 1. Equilibrium points of the diabatic 1B_2 PES of ozone.

Stationary Point	Order	r	R	γ	Energy
minimum	0	2.258	3.751	2.198	3.429
saddle-1	1	2.310	5.400	1.993	4.053
saddle-2	1	2.703	3.401	2.294	4.108
saddle-3	1	2.275	3.583	1.571	4.181
saddle-4	2	2.301	4.126	1.571	4.242
$O({}^1D)+O_2(a^1\Delta_g)$	2	2.316	∞	—	4.046

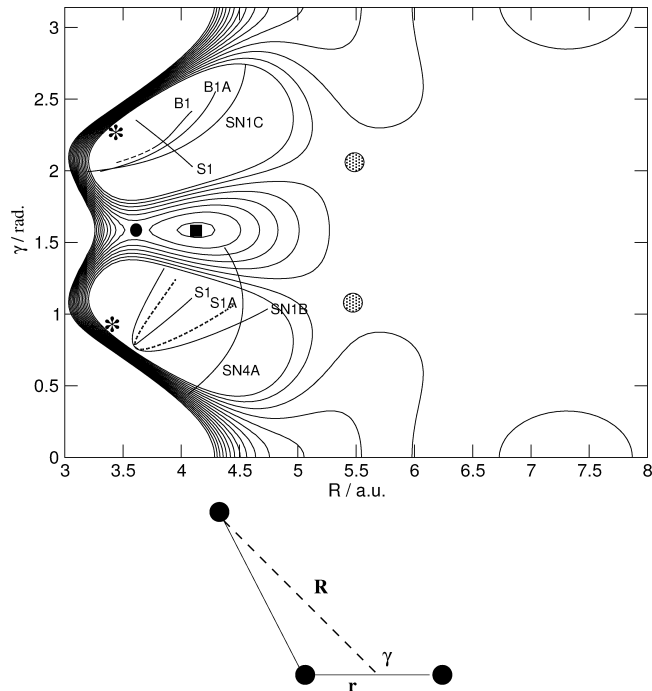


Fig. 12. Potential energy contours for the diabatic 1B_2 -state of ozone. Energies are in electronvolts, distances in Bohrs and the angle in radians. The energies cover the interval of (4.0–4.5) eV in 0.033 eV steps. The points shown on the graph mark the saddle points 1 (dotted circle), 2 (stars), 3 (filled circle) and 4 (filled square) (see Table 1). The periodic orbits overlaid are discussed in the text.

either symmetric or antisymmetric with respect to $\gamma' = 90^\circ$ (see Fig. 15). Therefore, results related to the quantum mechanical calculations will be presented in the symmetric-Jacobi coordinate system, otherwise in the following with Jacobi coordinates we mean the originally defined for the asymmetric geometry.

The selected grid parameters are $0.5 a_0 \leq R' \leq 3.0 a_0$ with 64 potential optimized points [Echave & Clary, 1992] and $3.0 a_0 \leq r' \leq 7.0 a_0$ with 64 potential optimized points. The angular coordinate is represented by 64 Gauss–Legendre quadrature points [Bacic & Light, 1989] in the interval $0 \leq \gamma' \leq 90^\circ$. Only those points are retained in the grid whose potential energy is smaller than 6.5 eV. Two types of calculations have been performed; Filter diagonalization [Grozdanov *et al.*, 1995; Wall & Neuhauser, 1995] and harmonic inversion [Mandelshtam & Taylor, 1997]. More details are given in [Qu *et al.*, 2004a, 2004b].

In Fig. 12, isopotential curves are depicted in the (R, γ) plane. The symbols on this picture mark the positions of the saddle points tabulated in Table 1. The saddle points which separate two

equivalent minima by exchanging their short and long bonds are denoted by stars. The geometry of this saddle is better portrayed in projections of the potential function in the plane with the two bond lengths of the molecule as coordinates shown in Fig. 1 of [Qu *et al.*, 2004a, 2004b]. Note the differences in the values of r for the saddle points. Except for saddle-4 which is of second order, i.e. it has two unstable directions with imaginary frequencies, all the other saddles are of single order. The stable degree of freedom for saddle-4 is the *short-bond* r as can be seen in Fig. 12 where this saddle point appears as a maximum.

The normal mode frequencies are estimated to be $\omega_3 = 1585 \text{ cm}^{-1}$ for the *short-bond* local mode, $\omega_1 = 743 \text{ cm}^{-1}$ for the *long-bond* local mode, and $\omega_2 = 400 \text{ cm}^{-1}$ for the bend. They are in an approximate $\omega_2 : \omega_1 : \omega_3 = 1 : 2 : 4$ resonance.

The evolution of the normal mode frequencies with increasing energy in a nonlinear potential is better represented in a projection of the continuation/bifurcation (C/B) diagram [Allgower & Georg, 1993] in the (E, ω) plane of those families of periodic orbits associated with the normal modes [Weinstein, 1973; Moser, 1976], named fundamental or principal families [Farantos, 1996; Ishikawa *et al.*, 1999; Joyeux *et al.*, 2002]. In Fig. 13 the three principal

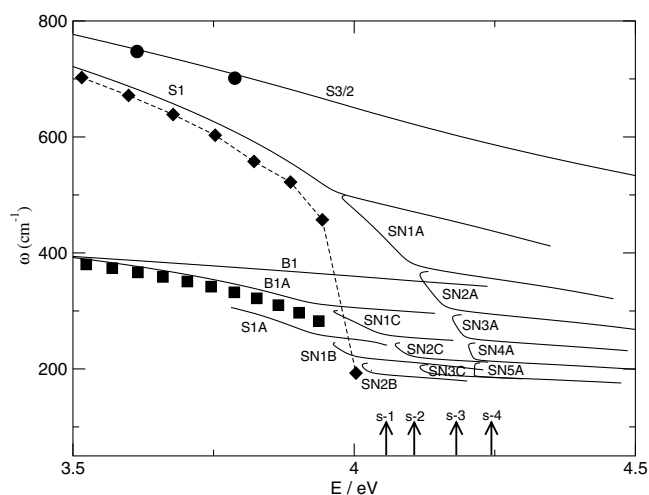


Fig. 13. C/B diagram of the 1B_2 -state of ozone. S1 denotes the *long-bond* mode, S1A its double period bifurcation. S3 the *short-bond* mode, B1 the bend mode and B1A an early saddle-node bifurcation of B1. The symbol SN denotes cascades of saddle-node bifurcations. SNiA is related with the S1 family, SNiB with S1A family whereas the SNiC with the B1A. The arrows mark the energies of the saddle points (s-i) in the potential. PO families related with the s-2 have not been located.

families of periodic orbits are shown and they are denoted as S1 for the *long-bond* stretch, B1 for the bend and S3 for the *short-bond* stretch. B1 exhibits an early saddle-node bifurcation, B1A, at about 3.475 eV with a tiny energy gap, whereas a double period bifurcation is found for the S1 (S1A) at about 3.78 eV. As we can see in this figure the three most anharmonic families, S1, S1A and B1A, develop cascades of saddle-node bifurcations as energy approaches the dissociation limit (saddle-1) for the SNiB, the saddle-3 for the SNiC cascade, and saddle-4 for the SNiA, respectively. We have not searched for the PO which point to the saddle-2. The saddle-node bifurcations are of similar type as found in the quartic potential. The frequency of the parent family levels off as energy approaches the critical energy where bifurcation occurs, with the appearance of a saddle-node bifurcation one branch of which inherits the characteristics of the parent family. The whole scenario is repeated at higher energies resulting in a cascade of such SN bifurcations. We do not distinguish the stability of the PO in this bifurcation diagram. In most cases the anharmonic branch is stable, at least for some energy, and the other branch is unstable, and therefore it is difficult to continue in energy. However, for a three-dimensional system, like ours, a SN bifurcation may show one single unstable and one double unstable branch instead, as is depicted in Fig. 11. For larger molecules with more degrees of freedom the number of combinations of course increases.

Representative PO at energies about 3.8 eV (if they exist) are depicted in Fig. 12. From this figure it becomes apparent that the double period bifurcation (S1A) and the SNiB families of PO are those which are directed towards the dissociation channel.

In Fig. 13 the point symbols denote the quantum mechanical frequencies obtained from the energy differences of adjacent eigenstates whose wave functions can be clearly assigned. They are state overtone progressions of the short-bond stretch (S3), bend (B1A) and long-bond stretch (S1). The corresponding eigenfunctions have well recognized nodal structures, and therefore the number of excitation quanta in each mode can easily be assigned as $(0, 0, v_3)$ for the S3 states, $(0, v_2, 0)$ for B1A and $(v_1, 0, 0)$ for the S1 states. In order to approximately account for the zero-point energy, the quantum results are shifted to lower energies by the zero-point energy. The energy differences are plotted with respect to the upper level.

Representative eigenfunctions with their assignment are shown in Fig. 14 and more in [Qu *et al.*, 2004a, 2004b]. The wave functions are plotted in symmetric Jacobi coordinates. The plots show the $|\Psi|^2$ for a specific iso-probability density surface viewed along γ' axis, in the direction perpendicular to the (r', R') plane. To see their correspondence to the periodic orbits which have been assigned, in Fig. 15 we plot the periodic orbits in the symmetric Jacobi (r', R') plane and for fixed angle $\gamma' = 111^\circ$. The ranges of the coordinate intervals are the same as in the wave functions.

In the symmetric Jacobi coordinates the S3 progression (short-bond mode) has mainly excitation along the perpendicular direction (γ'). The bend

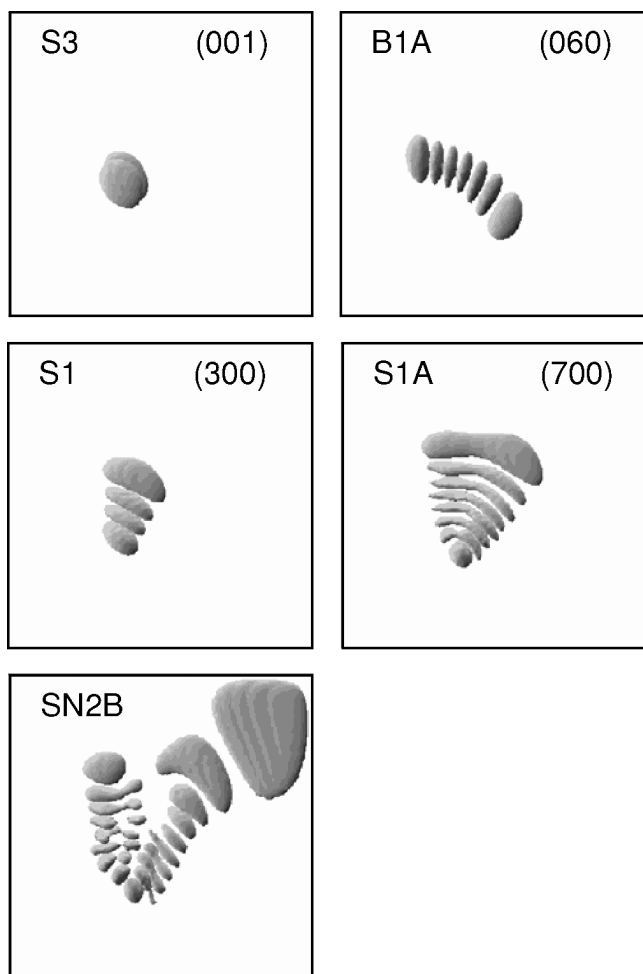


Fig. 14. Representative wave functions which show the characteristic localization in configuration space of the main overtone progressions. Symmetric Jacobi coordinates are used. The plots are viewed along the γ' axis, in the direction perpendicular to the (r', R') plane. The values of axes are for r' [3.0, 7.0] a.u. and R' [0.5, 3.0] a.u. Shading emphasizes the 3D character of the wave functions.

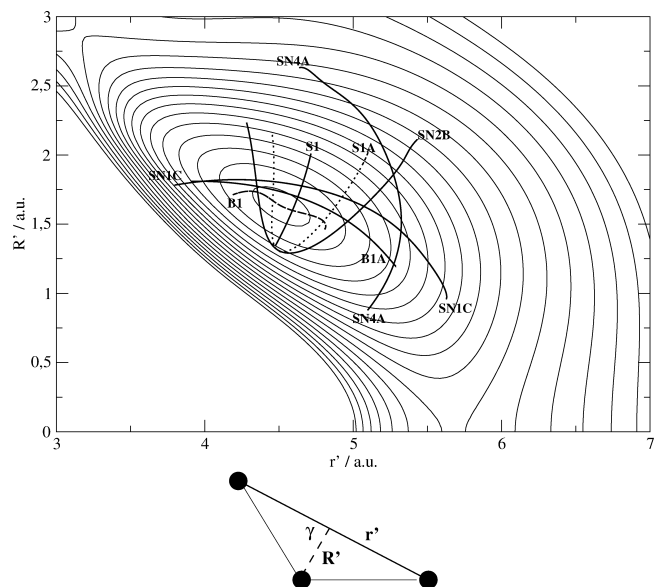


Fig. 15. Projection of the potential function and periodic orbits in the (r', R') plane in symmetric Jacobi coordinates. The angle γ' is kept fixed at 111° .

progression from the beginning is associated with the SN bifurcating family B1A and not with the principal bending family which is B1. As we can see in Fig. 13 there is a good agreement among the classical and quantum mechanical B1A frequencies for most of the assigned energies. However, differences are found for the S1 progression. These correspond to the long bond stretching states. The agreement among S1 PO and quantum frequencies is satisfactory up to four quanta of excitation (4, 0, 0). At the (5, 0, 0) state systematic mixing with another type of states sets in. Obviously, the (7, 0, 0) state shown in Fig. 14 is influenced from the double period bifurcation of the S1 family, S1A. This explains the deviation of the quantum frequencies from the classical curve S1, in Fig. 13.

Unfortunately, for higher energies the mixing in the wave functions becomes significant and that prohibits their visual assignment. However, we expect that wave functions which are directed towards the dissociation channel are associated with SN bifurcations and particularly with the SNiB families. Indeed, at energies close to the dissociation barrier we found localized eigenfunctions similar to the SNiB PO (see Fig. 14). It is difficult to assign adjacent levels for this family of states, and thus, the frequency of approximately 200 cm^{-1} given to this state in Fig. 13 is only an estimate.

In previous studies, such as HOCl [Weish *et al.*, 2000] and HOBr [Azzam *et al.*, 2003], the

association of quantum mechanical overtone progressions from the bottom of the well up to the dissociation threshold, with saddle-node bifurcations has clearly been shown. Recently, in a study of the $\text{CH}_2(\tilde{a}^1A_1)$ molecule we have found unequivocally assigned progressions of quantum states which lead above the isomerization and dissociation barriers [Farantos *et al.*, 2004; Lin *et al.*, 2005], and they also follow the tracks of SN bifurcations. The agreement is not only in the frequencies but also among periodic orbits and eigenfunctions.

The saddle-node bifurcations which approach an equilibrium point have the characteristics of the SN bifurcation observed in the two parameter quartic potential, i.e. it springs off a main family of PO with a gap in the energy. In the case of molecules the second parameter is generated from the coupling of the vibrational modes. Indeed, we can show that the cascade of SN bifurcations is the result of high order resonances between two vibrational modes. However, SN bifurcations are also found above the barriers of isomerization/dissociation [Farantos, 1996]. There is evidence that they result from the unstable periodic orbits originated from the saddle point and the Newhouse wild hyperbolic set [Newhouse, 1979; Borondo *et al.*, 1996; Contopoulos *et al.*, 1996]. These periodic orbits seem to have no connection to any main family and they appear abruptly like the cubic polynomial type.

The cubic and quartic models seem to fit with our experience in locating SN bifurcations in molecular Hamiltonians. The quartic type, those which are associated with a parent family, are found by monitoring the curvature of the continuation curve of the parent family. Continuation is carried out using the period as a parameter than the total energy. Then the derivatives $d\omega(E)/dE$ and $d^2\omega(E)/dE^2$ signal the approach to the critical energy of bifurcation. By giving a proper increment to the period we overcome the gap and join the branch of the SN family which is the continuation of the parent family. In the continuation scheme the starting initial conditions are those of a periodic orbit before the gap with period T_0 and then POMULT converges to a new PO with a period $T_0 + \Delta T$ in one of the two branches of SN bifurcation. This is how we can find several members in a cascade of SN bifurcations.

The cubic type is not associated with a parent family but it appears in the neighborhood of stable/unstable entanglements of a principal unstable periodic orbit which always exist above saddle

points of the potential [Moser, 1976]. Thus, we initially propagate the stable and the unstable manifolds for some energies, and then search for low order periodic orbits in their neighborhood.

5. Conclusions

Figure 4 shows the typical phase space structure close to the SN bifurcation of a 1-D one parameter cubic potential; a stable region surrounded by unstable trajectories. This reveals the importance of saddle-node bifurcations. Their sudden appearance in phase space with increasing energy may create stable regions even if the dynamics is chaotic at lower energies. If the stability region is comparable to the volume of \hbar^N , then semiclassically we expect the localization of an eigenfunction. The SN elementary bifurcation is generic and robust, perturbations in the potential do not vanish a SN bifurcation, as in the cubic potential the introduction of one additional parameter ($\alpha \neq 0$) does not change the structure of the phase space. For molecules we have found two kinds of saddle-node bifurcations of periodic orbits. The first kind is associated to a parent family. The second seems to be related to the stable and unstable manifolds of unstable periodic orbits.

Another important elementary bifurcation is the Hamiltonian–Hopf bifurcation [van der Meer, 1985] which is encountered in three-dimensional systems and in systems with higher dimensionality. A Hopf-like bifurcation is expected when the two pairs of eigenvalues of the monodromy matrix are out of the unit complex circle (see Fig. 11). Acetylene is one example for which such bifurcations have been found [Contopoulos *et al.*, 1994; Prosmiiti & Farantos, 1995]. In the future we plan to investigate further Hopf-like bifurcations in relation to the dynamics and spectroscopy of molecules.

Acknowledgments

Support from the Greek Ministry of Education and European Union through the postgraduate program EPEAEK, “Applied Molecular Spectroscopy”, is gratefully acknowledged.

References

- Allgower, E. L. & Georg, K. [1993] *Numerical Continuation Methods*, Springer Series in Computational Mathematics, Vol. 13 (Springer-Verlag, Berlin).

- Arnold, V. I. [1980] *Mathematical Methods of Classical Mechanics*, Graduate Text in Mathematics, Vol. 60 (Springer-Verlag).
- Azzam, T., Schinke, R., Farantos, S. C., Joyeux, M. & Peterson, K. A. [2003] "The bound state spectrum of HOBr up to dissociation limit: Evolution of saddle-node bifurcations," *J. Chem. Phys.* **118**, 9643–9652.
- Bacic, Z. & Light, J. C. [1989] "Theoretical methods for rovibrational states of floppy molecules," *Ann. Rev. Phys. Chem.* **40**, 469–498.
- Berry, M. V. & Tabor, M. [1977] "Calculating the bound spectrum by path summation in action-angle variables," *J. Phys. A* **10**, 371–379.
- Borondo, F., Zembekov, A. A. & Benito, R. M. [1996] "Saddle-node bifurcations in the LiNC/LiCN molecular system: Classical aspects and quantum manifestations," *J. Chem. Phys.* **105**, 5068–5081.
- Contopoulos, G., Farantos, S. C., Papadaki, H. & Polymilis, C. [1994] "Complex unstable periodic orbits and their manifestation in classical and quantum dynamics," *Phys. Rev. E* **50**, 4399–4403.
- Contopoulos, G., Grousouzakou, E. & Polymilis, C. [1996] "Distributions of periodic orbits and the homoclinic tangle," *Cel. Mech. Dyn. Astron.* **64**, 363–381.
- Crawford, J. D. [1991] "Introduction to bifurcation theory," *Rev. Mod. Phys.* **63**, 991–1037.
- Crim, F. F. [1999] "Vibrational state control of bimolecular reactions: Discovering and directing the chemistry," *Acc. Chem. Res.* **32**, 877–884.
- Dai, H.-L. & Field, R. W. [1995] *Molecular Dynamics and Spectroscopy by Stimulated Emission Pumping* (World Scientific, Singapore).
- Delon, A., Reiche, F., Abel, B., Grebenshchikov, S. Yu. & Schinke, R. [2000] "Investigation of loosely bound states of NO₂ just below the first dissociation threshold," *J. Phys. Chem.* **104**, 10374–10382.
- Echave, J. & Clary, D. C. [1992] "Potential optimized discrete variable representation," *Chem. Phys. Lett.* **190**, 225–230.
- Farantos, S. C. [1992] "Chemical dynamics: A periodic orbits approach," in *Time Dependent Quantum Mechanics: Experiments and Theory*, eds. Broeckhove, J. & Lathouwers, L., NATO Advanced Science Institutes Series B: Physics, Vol. 299 (Plenum Co. Ltd), pp. 27–43.
- Farantos, S. C. [1993] "Periodic orbits as a probe to reveal exotic states: The saddle-node states," *Laser Chem.* **13**, 87–99.
- Farantos, S. C. [1996] "Exploring molecular vibrations with periodic orbits," *Int. Rev. Phys. Chem.* **15**, 345–374.
- Farantos, S. C. [1998] "POMULT: A program for computing periodic orbits in Hamiltonian systems based on multiple shooting algorithms," *Comp. Phys. Comm.* **108**, 240–258.
- Farantos, S. C., Lin, D. Y. & Guo, H. [2004] "A regular isomerization path among chaotic vibrational states of CH₂(\bar{a}^1A_1)," *Chem. Phys. Lett.* **399**, 260–265.
- Flach, S. & Willis, C. R. [1998] "Discrete breathers," *Phys. Rep.* **295**, 181–264.
- Founargiotakis, M., Farantos, S. C., Skokos, H. & Contopoulos, G. [1997] "Bifurcation diagrams of periodic orbits for unbound molecular systems: FH₂," *Chem. Phys. Lett.* **277**, 456–464.
- Grozdanov, T. P., Mandelshtam, V. A. & Taylor, H. S. [1995] "Recursion polynomial expansion of the Green's function with absorbing boundary conditions: Calculations of resonances of HCO by filter diagonalization," *J. Chem. Phys.* **103**, 7990–7995.
- Guantes, R., Nezis, A. & Farantos, S. C. [1999] "Periodic orbit — quantum mechanical investigation of the inversion mechanism of Ar₃," *J. Chem. Phys.* **111**, 10836–10842.
- Guckenheimer, J. & Holmes, P. [1983] *Nonlinear Oscillations, Dynamical Systems, and Bifurcations of Vector Fields* (Springer-Verlag, Berlin).
- Gutzwiller, M. C. [1990] *Chaos in Classical and Quantum Mechanics*, Vol. 1 (Springer-Verlag).
- Halonen, L. [1998] "Local mode vibrations in polyatomic molecules," *Adv. Chem. Phys.* **104**, 41–179.
- Heller, E. J. [1984] "Bound-state eigenfunctions of classically chaotic Hamiltonian systems: Scars of periodic orbits," *Phys. Rev. Lett.* **53**, 1515–1518.
- Herman, M., Lievin, J. & Auwera, J. V. [1999] "Global and accurate vibration Hamiltonians from high-resolution molecular spectroscopy," *Adv. Chem. Phys.* Vol. 108 (John Wiley and Sons, Inc.), pp. 1–431.
- Houston, P. L. [2003] "Photodissociation dynamics of ozone in the Hartley band," in *Modern Trends in Chemical Dynamics*, eds. Yang, X. & Liu, K., Advanced Series in Physical Chemistry, Vol. 14 (World Scientific, Singapore), p. 197.
- Ishikawa, H., Nagao, C., Mikami, N. & Field, R. W. [1998] "Spectroscopic investigation of the generation of 'isomerization' states: Eigenvector analysis of the bend-CP stretch polyad," *J. Chem. Phys.* **109**, 492–503.
- Ishikawa, H., Field, R. W., Farantos, S. C., Joyeux, M., Koput, J., Beck, C. & Schinke, R. [1999] "HCP \leftrightarrow CPH isomerization: Caught in the act," *Ann. Rev. Phys. Chem.* **50**, 443–484.
- Jacobson, M. P., O'Brien, J. P. & Field, R. W. [1998a] "Anomalously slow intramolecular vibrational redistribution in the acetylene $\bar{X}^1\Sigma_g^+$ state above 10000 cm⁻¹ of internal energy," *J. Chem. Phys.* **109**, 3831–3840.
- Jacobson, M. P., O'Brien, J. P., Silbey, R. J. & Field, R. W. [1998b] "Pure bending dynamics in the acetylene $\bar{X}^1\Sigma_g^+$ state up to 15000 cm⁻¹ of internal energy," *J. Chem. Phys.* **109**, 121–133.

- Jacobson, M. P., Silbey, R. J. & Field, R. W. [1999] "Local mode behavior in the acetylene bending system," *J. Chem. Phys.* **110**, 845–859.
- Jonas, D. M., Solina, S. A. B., Rajaram, B., Silbey, R. J., Field, R. W., Yamanouchi, K. & Tsuchiya, S. [1993] "Intramolecular vibrational redistribution of energy in the stimulated emission pumping spectrum of acetylene," *J. Chem. Phys.* **99**, 7350–7370.
- Joyeux, M., Farantos, S. C. & Schinke, R. [2002] "Highly excited motion in molecules: Saddle-node bifurcations and their fingerprints in vibrational spectra," *J. Phys. Chem.* **106**, 5407–5421.
- Joyeux, M., Grebenshchikov, S. Yu, Bredenbeck, J., Schinke, R. & Farantos, S. C. [2005] "Intramolecular dynamics along isomerization and dissociation pathways," in *Geometrical Structures of Phase Space in Multi-Dimensional Chaos*, Adv. Chem. Phys. Vol. 130, pp. 267–303.
- Keller, H.-M., Flöthmann, H.-M., Dobbyn, A. J., Schinke, R., Werner, H.-J., Bauer, C. & Rosmus, P. [1996] "The unimolecular dissociation of HCO. II. Comparison of calculated resonance energies and widths with high-resolution spectroscopic data," *J. Chem. Phys.* **105**, 4983–5004.
- Keller, H.-M., Stumpf, M., Schröder, T., Stöck, C., Temps, F., Schinke, R., Werner, H.-J., Bauer, C. & Rosmus, P. [1997] "Unimolecular dissociation dynamics of highly vibrationally excited DCO(\tilde{X}^2A). II. Calculation of resonance energies and widths and comparison with high-resolution spectroscopic data," *J. Chem. Phys.* **106**, 5359–5378.
- Kopidakis, G. & Aubry, S. [1999] "Intraband discrete breathers in disordered nonlinear systems. I. Delocalization," *Physica D* **130**, 155–309.
- Lawton, R. T. & Child, M. S. [1981] "Local and normal stretching vibrational states of H₂O classical and semiclassical considerations," *Mol. Phys.* **44**, 709–723.
- Light, J. C. & Carrington, T. [2000] "Discrete-variable representations and their utilization," *Adv. Chem. Phys.* **114**, 263–310.
- Lin, S. Y., Guo, H. & Farantos, S. C. [2005] "Resonance states of CH₂(\tilde{a}^1A_1) and their roles in unimolecular and bimolecular reactions," *J. Chem. Phys.* **122**, 124308.
- Mandelshtam, V. A. & Taylor, H. S. [1997] "A low-storage filter diagonalization method for quantum eigenenergy calculations or for spectral analysis of time signals," *J. Chem. Phys.* **106**, 5085–5090.
- Moser, J. [1976] "Periodic orbits near an equilibrium and a theorem by Alan Weinstein," *Commun. Pure Appl. Math.* **29**, 727–747.
- Newhouse, S. E. [1979] "The abundance of wild hyperbolic sets and non-smooth stable sets for diffeomorphisms," *Publ. Math. IHES* **50**, 101–151.
- Northrup, F. J., Bethardy, G. A. & Macdonald, R. G. [1997] "Infrared absorption spectroscopy of HNC in the region 2.6 to 3.1 μm ," *J. Mol. Spectrosc.* **186**, 349–362.
- Ozorio de Almeida, A. M. [1990] *Hamiltonian Systems: Chaos and Quantization* (Cambridge University Press, NY).
- Prosimiti, R. & Farantos, S. C. [1995] "Periodic orbits, bifurcation diagrams and the spectroscopy of C₂H₂ system," *J. Chem. Phys.* **103**, 3299–3314.
- Prosimiti, R., Farantos, S. C. & Guo, H. [1999] "Assigning the transition from normal to local vibrational mode in SO₂ by periodic orbits," *Chem. Phys. Lett.* **311**, 241–247.
- Prosimiti, R. & Farantos, S. C. [2003] "Periodic orbits and bifurcation diagrams of acetylene/vinylidene revisited," *J. Chem. Phys.* **118**, 8275–8280.
- Qu, Z. W., Zhu, Schinke, R. & Farantos, S. C. [2004a] "The Huggins band of ozone: A theoretical analysis," *J. Chem. Phys.* **121**, 11731–11745.
- Qu, Z. W., Zhu, H., Tashiro, M., Schinke, R. & Farantos, S. C. [2004b] "The Huggins band of ozone: Unambiguous electronic and vibrational assignment," *J. Chem. Phys.* **120**, 6811–6814.
- Sako, T. & Yamanouchi, K. [1996] "Algebraic approach to vibrationally highly excited states of SO₂. Vibrational wavefunctions from spectroscopy," *Chem. Phys. Lett.* **264**, 403–410.
- Stamatiadis, S., Prosimiti, R. & Farantos, S. C. [2000] "AUTO_DERIV: Tool for automatic differentiation of a FORTRAN code," *Comp. Phys. Comm.* **127**, 343–355.
- van der Meer, J.-C. [1985] *The Hamiltonian Hopf Bifurcation*, Vol. 1160 (Springer-Verlag, NY).
- Wall, M. R. & Neuhauser, D. [1995] "Extraction, through filter-diagonalization, of general quantum eigenvalues or classical normal mode frequencies from a small number of residues or a short-time segment of a signal. I. Theory and application to a quantum-dynamics model," *J. Chem. Phys.* **102**, 8011–8022.
- Weinstein, A. [1973] "Normal modes for nonlinear Hamiltonian systems," *Inv. Math.* **20**, 47–57.
- Weish, J., Hauschildt, J., Düren, R., Schinke, R., Koput, J., Stamatiadis, S. & Farantos, S. C. [2000] "Saddle-node bifurcations and their quantum mechanical fingerprints in the spectrum of HOCl," *J. Chem. Phys.* **112**, 77–93.
- Wiggins, S. [2003] *Introduction to Applied Nonlinear Dynamical Systems and Chaos*, Second Edition (Springer-Verlag, NY).
- Xie, A., van der Meer, L., Hoff, W. & Austin, R. H. [2000] "Long-lived amide I vibrational modes in myoglobin," *Phys. Rev. Lett.* **84**, 5435–5438.
- Yakubovich, V. A. & Starzhinskii, V. M. [1975] *Linear Differential Equations with Periodic Coefficients*, Vol. 1 (Halsted Press).

- Yamamoto, T. & Kato, S. [1998] "Quantum dynamics of unimolecular dissociation reaction $\text{HF} + \text{CO} \rightarrow \text{HF} + \text{CO}$," *J. Chem. Phys.* **109**, 9783–9794.
- Yamanouchi, K., Yamada, H. & Tsuchiya, S. [1988] "Vibrational level structure of highly excited SO_2 in the electronic ground state as studied by stimulated emission pumping spectroscopy," *J. Chem. Phys.* **88**, 4664–4670.
- Yamanouchi, K., Takeuchi, S. & Tsuchiya, S. [1990] "Vibrational level structure of highly excited SO_2 in the electronic ground state. II. Vibrational assignment by dispersed fluorescence and stimulated emission pumping spectroscopy," *J. Chem. Phys.* **92**, 4044–4054.
- Zou, S. & Bowman, J. M. [2002] "Full dimensionality quantum calculations of acetylene/vinylidene isomerization," *J. Chem. Phys.* **117**, 5507–5510.